Earth and Planetary Science Letters 284 (2009) 386–391

Contents lists available at ScienceDirect

Earth and Planetary Science Letters

journal homepage: www.elsevier.com/locate/epsl

Significant effect of grain size distribution on compaction rates in granular aggregates

André Niemeijer [a,b,c,*], Derek Elsworth [a,c], Chris Marone [b,c]

[a] Department of Energy and Mineral Engineering, The Pennsylvania State University, USA
[b] Department of Geosciences, The Pennsylvania State University, USA
[c] G3 Center and Energy Institute, The Pennsylvania State University, USA

ARTICLE INFO

Article history:
Received 6 December 2008
Received in revised form 14 April 2009
Accepted 30 April 2009
Available online 28 May 2009

Editor: L. Stixrude

Keywords:
compaction
grain size
pressure solution

ABSTRACT

We investigate the role of pressure solution in deformation of upper- to mid-crustal rocks using aggregates of halite as a room temperature analog for fluid-assisted deformation processes in the Earth's crust. Experiments evaluate the effects of initial grain size distribution on macroscopic pressure solution rate of the aggregate and compare the results to theoretical models for pressure solution. We find that the grain size exponent deviates significantly from the theoretical value of 3 for diffusion-controlled pressure solution. Models typically assume mono-dispersed spherical particles in pseudo-regular packing. We infer that the discrepancy between experimentally determined grain size exponents and the theoretical values are a result of deviation of experimental (and natural) samples from regular packs of mono-dispersed spherical particles. Moreover, we find that compaction rates can vary by up to one order of magnitude as a function of the width of the grain size distribution for a given mean grain size. Wider size distributions allow for higher initial compaction rates, increasing the macroscopic compaction rate with respect to more narrow grain size distributions. Grain sizes in rocks, fault gouges, and hydrocarbon reservoirs are typically log-normal or power law distributed and therefore pressure solution rates may significantly exceed theoretical predictions. Spatiotemporal variations in pressure solution rates due to variations in grain size may cause the formation of low porosity zones, which could potentially focus deformation in these zones and produce pockets of high pore pressures, promoting nucleation of frictional instability and earthquake rupture.

1. Introduction

Fluids are ubiquitous in the Earth's crust and play an important role in the evolution of fluid reservoirs, the development and migration of oil, gas and ore deposits and in the seismic cycle (i.e. fault healing, sealing, pore pressure evolution). Pressure solution is the serial process of dissolution of material at stressed grain contacts, diffusion of this material out of the grain contact and subsequent transport via the pore fluid or precipitation on the pore walls. Much experimental and modeling work has been done to investigate the process of pressure solution (e.g. Rutter, 1976; Rutter, 1983; Spiers et al., 1990; Mullis, 1991; Schutjens, 1991; Gratier, 1993; Dewers and Hajash, 1995; Shimizu, 1995; Renard et al., 1999; Gundersen et al., 2002; Niemeijer et al., 2002; Yasuhara et al., 2003; Spiers et al., 2004; Revil et al., 2006; Bernabé and Evans, 2007; Fitzenz et al., 2007). Despite these efforts, there is still considerable discrepancy between experimental and modeling results. The disagreement is primarily in the rate limiting mechanism (i.e. diffusion, dissolution, or precipitation) under varying conditions of pressure, temperature and grain size, because knowledge of the mechanistic kinetics at grain contacts is limited (especially for diffusion). Moreover, typical models of pressure solution assume an idealized grain shape and packing geometry, which complicates comparison between models and experimental results. It is also difficult to truly isolate pressure solution as the single deformation mechanism in experimental work. Indeed, the operation of fluid-assisted stress corrosion crack and/or dislocation creep at highly stressed contacts can not be excluded. Finally, experimental studies have generally assumed an idealized set of monodisperse grains, rather than an aggregate with a distribution of sizes, and thus comparison between experimental grain size dependence and theory is problematic. Indeed, few experimental studies find values for the grain size dependence that are close to the values predicted by theory (e.g. Raj, 1982; Spiers et al., 1990; Spiers and Brzesowsky, 1993; Shimizu, 1995).

It has been well established that pressure solution compaction in salt aggregates is extremely rapid at room temperature conditions. This is due to the high solubility of salt in water and the rapid kinetics of the dissolution and precipitation reactions. Therefore, salt is a suitable analogue for the study of pressure solution in common rock-forming minerals (e.g. quartz) under upper- to mid-crustal hydrothermal conditions.

The purpose of this paper is to present results from laboratory experiments in which we evaluate the effect of grain size distribution on the macroscopic compaction rate of a granular aggregate. We do

* Corresponding author. Istituto Nazionale di Geofisica e Volcanologia, Via di Vigna Murata 605, Roma, Italy.
E-mail address: arn3@psu.edu (A. Niemeijer).

0012-821X/$ – see front matter © 2009 Elsevier B.V. All rights reserved.
doi:10.1016/j.epsl.2009.04.041

Table 1
List of experiments performed.

Experiment	Sieve fraction (μm)	Starting porosity	Final porosity	Total volumetric strain
p1477	38–53	45.22	1.87	0.44
p1478	53–106	44.62	6.91	0.41
p1479	38–106	40.85	3.44	0.39
p1480	106–212	43.74	9.01	0.38
p1647	63–90	41.11	9.52	0.35
p2014	38–53 and 106–12	37.23	0.60	0.37
p2030	63–90	39.61	0.59	0.39

Normal stress was 5 MPa in all experiments.

not review existing models for pressure solution, but instead propose that one of the explanations for the discrepancy between models and experiments could be found in the presence of a distributed grain size. From our experiments, we conclude that the presence of small grains in a wide grain size distribution increase pressure solution rates by up to one order of magnitude compared to theory. Moreover, the derived grain size exponent deviates significantly from the theoretical value of 3 for diffusion-controlled pressure solution. Because grain sizes are usually distributed in natural rocks, locally higher pressure solution rates could have significant implications for fluid flow and localized deformation in fault zones and other settings where spatial variations in sorting exist.

2. Theory of pressure solution

Pressure solution is a serial set of processes and therefore the slowest process limits the overall reaction rate. The driving force of pressure solution is a stress gradient along the contact junction, which produces a gradient in chemical potential of components within the solid. The difference between the chemical potential at the grain contact and that at the pore wall can be written:

$$\Delta\mu_n = (\sigma_n - P_f)\Omega_s \tag{1}$$

for a representative elementary volume and neglecting changes in Helmholtz free energy. Here, μ_n is the chemical potential of the solid, σ_n is the normal stress at the grain boundary, P_f is the fluid pressure in the pore wall and Ω_s is the molar volume of the solid. Using the standard relation for the chemical potential of a dissolved solid and its concentration in an ideal solution, the difference in solubility of the solid for the stressed and unstressed cases can be written:

$$\Delta\mu_n = RT\,ln((C_s + \Delta C)/C_s) \approx RT(\Delta C/C_0) \tag{2}$$

Here, R is the universal gas constant, T is the absolute temperature, C_s is the concentration of the solid at the pore wall, which is taken to be equal to the concentration of the solid under purely hydrostatic stress, C_0, and ΔC is the enhancement of solubility at the grain contact relative to that at the pore wall. A common assumption is that the steady state deformation rate for pressure solution is controlled by the slowest of the three serial mechanisms of dissolution, diffusion and precipitation. In this case, it can be assumed that the total difference in chemical potential is consumed by this rate-controlling mechanism. In the case of salt at room temperature, it has been shown that diffusion is the rate-limiting mechanism (Spiers and Schutjens, 1990; Spiers et al., 1990). Therefore, we can relate the rate of pressure solution to the Fickian diffusive flux through the grain boundary, given by:

$$J_{gb} = -(DC\Omega/RT)\nabla\mu_{gb} \tag{3}$$

Here, D is the diffusion coefficient, C is the concentration of the solute in the grain boundary fluid and $\nabla\mu_{gb}$ is the gradient of chemical potential. Integrating Eq. (3) and combining with Eq. (1) gives the total diffusive flux of material out of the grain boundary in m^3/s, ignoring radial variations in $\nabla\mu_{gb}$ Dividing this flux over the area of the contact gives the convergence velocity of two grains:

$$J = \frac{\rho_f D_{gb}\delta C_0 \sigma_n \Omega_s}{d^2 \rho_s RT}. \tag{4}$$

The compaction rate (i.e. volumetric strain rate) for a porous aggregate depends on aggregate geometry and packing and particle shape (Rutter, 1976; Raj, 1982; Rutter, 1983; Spiers and Schutjens, 1990). Typically, a close-packed (face-centered cubic) array of identical spherical grains is assumed, which leads to the following relation between volumetric strain rate and volumetric strain

$$\dot{\varepsilon} = Z\frac{\sigma_n^e(1-\varepsilon_v)}{d^p\varepsilon_v^n}. \tag{5}$$

Here, Z contains all the kinetic parameters for the rate-limiting mechanism and p is the "grain size exponent" which is 3 for diffusion-controlled pressure solution. Now, for spherical grains and uniaxial compaction, n takes the value of 1, whereas for cubical grains the value of n is 2 (Schutjens, 1991). Note that Eq. (5) assumes: 1) that all the contacts converge at the same rate (i.e. hydrostatic strain), which is incorrect for an aggregate with a distributed grain size, and 2) that net strains remain less than 20%. Moreover, in deriving Eq. (5), it is assumed that no energy is consumed in grain boundary sliding. Spiers and Schutjens (1990) note that different packing geometries *for spherical grains* affect the volumetric strain rates by a factor less than 2. Although this change may seem small, it represents a problem when one compares volumetric strain rates from experiments with varying grain size and non-spherical grains.

3. Experimental methods

We conducted room temperature experiments on crushed rock salt, which was sieved into 5 different size ranges (Table 1). For each range we determined the grain size distribution using a laser diffraction Malvern Particle Sizer. The experiments were run in a double-direct shear apparatus (Fig. 1). The sample assembly consists of two forcing blocks (contact area 5×5 cm) that sandwich a center block, all with grooves machined on their loading surfaces. In each experiment, about 20 g of material were loaded on each side block to create two gouge layers with an initial thickness of ~10 mm each. The thickness of the entire assembly was measured on the bench and in-situ, in the testing apparatus, under load using digital calipers with a resolution of 0.01 mm.

All samples were compacted room-dry at 5 MPa for 15 min. Normal stress was applied to the sample via servo-control by driving the horizontal ram under load-feedback control (Fig. 1). Forces were measured using load cells with resolution of 0.1 kN (equivalent to ~0.04 MPa). Displacement of the vertical and horizontal pistons was

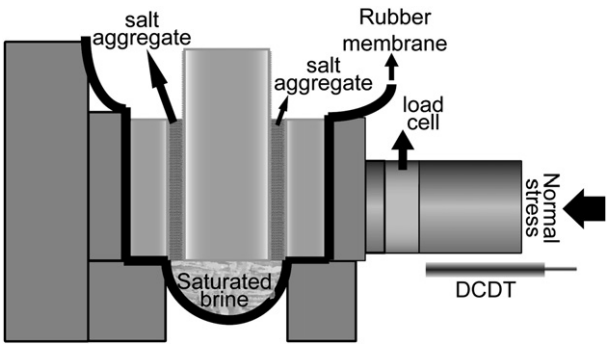

Fig. 1. Schematic diagram of the experimental set-up.

measured using displacement transducers with a resolution of 0.1 μm. Displacement and load were continuously recorded at a rate of 10 kHz and averaged to a rate of 1 Hz. After the initial dry compaction, the sample assembly was removed from the loading frame and its

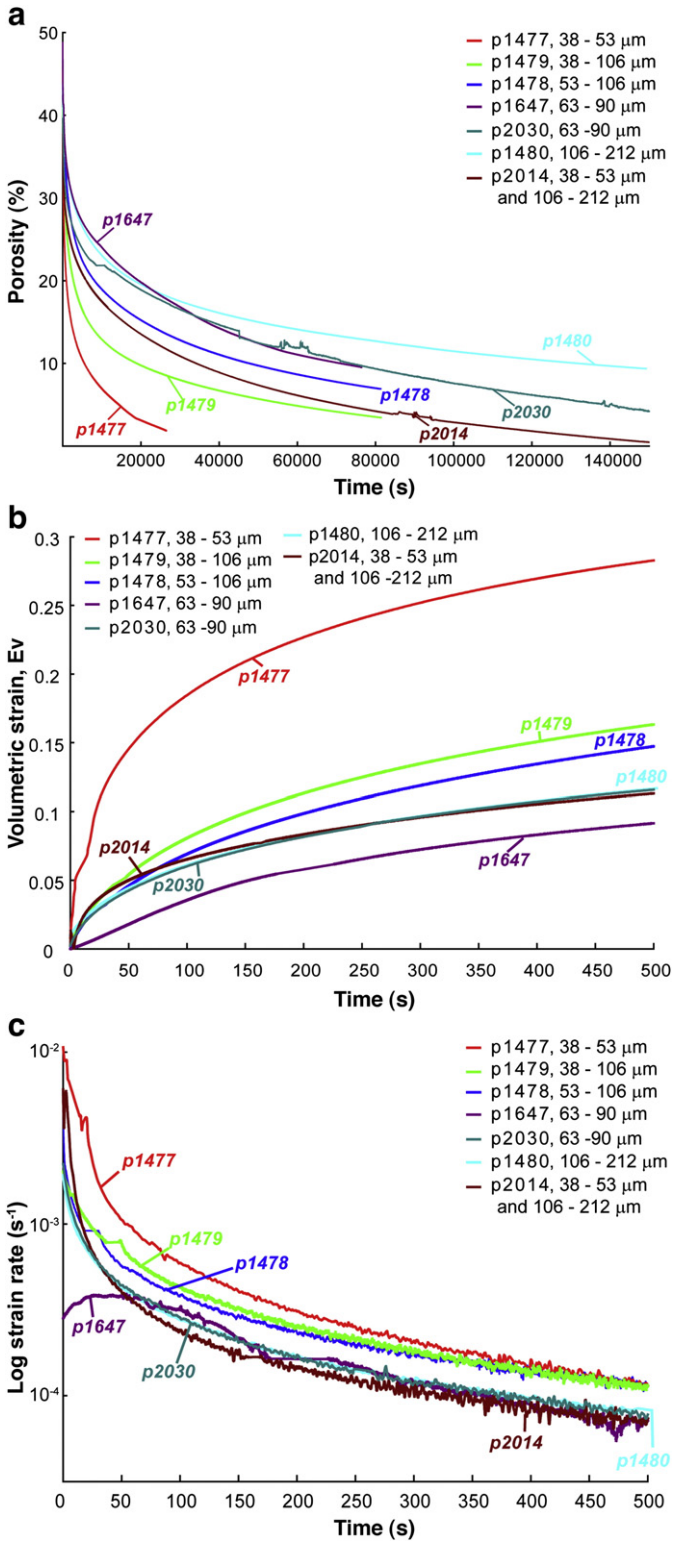

Fig. 2. a) Plot of evolution of porosity with time for all experiments. Normal stress is 5 MPa in all cases. Note that all samples were compacted dry for 15 min and left to saturate for 45 min prior to wet compaction (except sample p1647, which was not left to saturate). b) Plot of the evolution of volumetric strain with time for the initial 500 s of all experiments. c) Semi-log plot of the evolution of volumetric strain rate with time for the initial 500 s of all experiments.

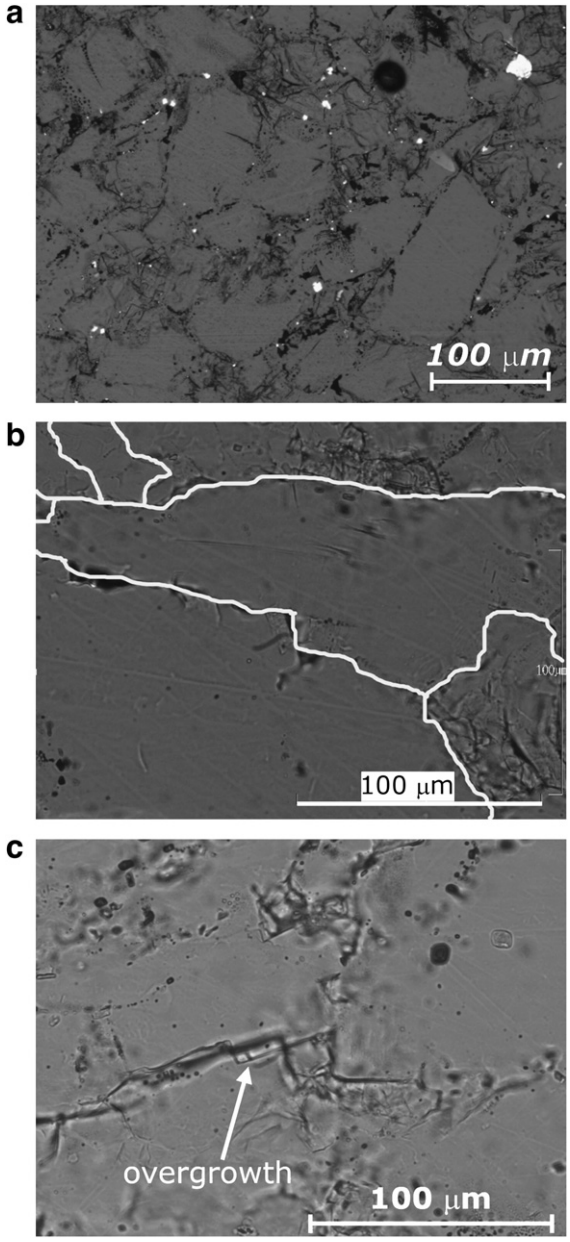

Fig. 3. a) Microscope image using plane polarized light of sample p1480, showing low porosity (~10%). Note the absence of inter- or intragranular cracks. b) Detail of the microstructure of sample p1480, showing long grain boundaries and grain-to-grain indentations. c) Detail of the microstructure of sample p1480, showing the presence of a salt overgrowth.

thickness was re-measured. The sample was then re-installed in the apparatus with a rubber bag placed around the sample assembly which was subsequently filled with brine, saturated with respect to the granular aggregate. The sample was allowed to saturate with fluid for 45 min (except for experiment p1647, which was loaded to 5 MPa directly after adding the saturated brine), after which a normal stress of 5 MPa was again applied. Porosity change was determined from measured initial sample mass and layer thickness and the change in layer thickness was derived from the movement of the horizontal piston at constant normal stress (i.e. assuming compaction occurs only in the layer-normal or horizontal direction). At the end of the experiment, the load was removed and the sample assembly removed from the loading frame. The side blocks were carefully removed from the center block and the compacted sample was removed from the forcing block using a razor blade and/or tapping of the block. Samples were then flushed with iso-butanol to remove any excess brine and

dried in an oven at 50 °C for 24 h after which they were impregnated with epoxy resin (Buehler company). Standard thin sections for microscope study were cut and prepared using iso-butanol as lubricant.

4. Results

In Fig. 2a, we show the porosity evolution of all experiments (data of final porosities are listed in Table 1). Room-dry compaction was negligible and is not shown. Fig. 2a shows strong initial compaction for all experiments, with porosity dropping to 25% or less within the first 20 min. Total compaction and initial compaction rate are highest for the finest grain size fraction (p1477, 38–53 μm) and lowest for the coarsest grain size fraction (p1480, 106–212 μm). In Fig. 2b, we show the porosity-derived volumetric strain as a function of time for the very initial part (500 s) of the experiments. All experiments show rapid initial compaction with varying time derivatives. This can be seen more clearly in Fig. 2c, where we show the volumetric strain rates (i.e. the slopes in Fig. 2b) *vs.* time in a semi-log plot. Initial strain rates are extremely rapid for samples p1477 and p2014, but decrease faster for sample p2014 (bi-modal grain size distribution, see also Table 1). Initial strain rate is lowest for sample p1647, which was not pre-saturated in contrast to sample p2030.

In Fig. 3, we show representative microstructures of the compacted samples. Fig. 3a shows an overview of the general microstructures, showing low porosity and indistinct grain boundaries. The grain size appears to reflect the initially sieved grain size fraction and no inter- or intragranular fractures are obvious, indicating that grain fracturing and size reduction was either absent or minor in our experiments. Fig. 3b shows long grain boundaries and indentations of neighboring grains. Finally, in Fig. 3c, we show the presence of a halite overgrowth (cubical structure) on an original salt grain, which clearly indicates the operation of a fluid-assisted deformation process, i.e. intergranular pressure solution.

5. Discussion

Our microstructural evidence shows that pressure solution is the dominant compaction mechanism, although a minor contribution of stress corrosion cracking and/or dislocation creep at the grain boundary cannot be excluded. Especially on the scale of highly stressed point contacts inside the grain boundary, it is likely that some dislocation creep or micro-cracking facilitated the dissolution of material. However, the macroscopic rate of porosity reduction is most likely controlled by pressure solution.

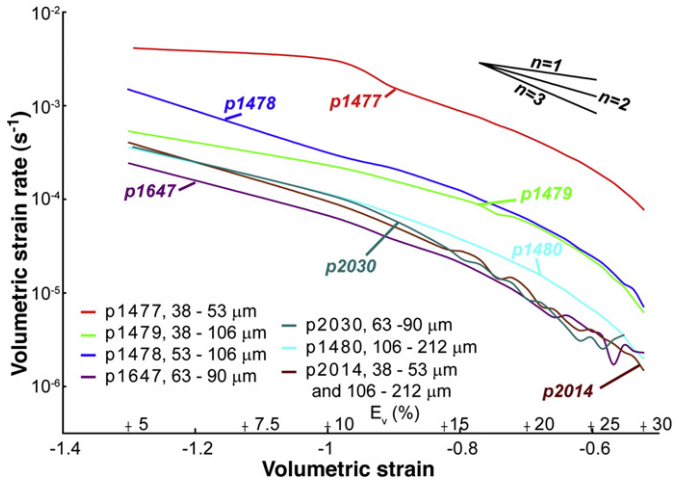

Fig. 4. Log–log plot of volumetric strain vs. strain rates for the entire suite of experiments. Data was averaged over an interval of 30 records (= 30 s in most cases) for steps in volumetric strain of 1%.

Table 2
Log-linear best fits of strain rate *vs.* strain for all experiments and varying ranges of volumetric strain.

Experiment	Range of volumetric strain (%)							
	0–10	0–15	0–20	0–25	0–30	10–20	5–15	10–30
p1477	−0.30	−0.37	−0.77	−1.21	−1.85	−2.68	−1.30	−3.56
p1478	−0.65	−0.91	−1.12	−1.30	−1.98	−1.90	−1.50	−3.36
p1479	−0.67	−0.97	−1.37	−1.90	−2.73	−2.45	−1.63	−4.05
p1480	−1.18	−1.56	−1.73	−2.20	−2.90	−2.62	−2.03	−3.80
p1647	−1.36	−1.72	−2.07	−2.57	−2.81	−2.89	−1.90	−3.31
p2014	−1.36	−1.89	−2.53	−3.36	−3.47	−4.15	−2.39	−4.45
p2030	−1.38	−1.85	−2.59	−3.31	−2.62	−3.75	−2.34	−2.63

5.1. Evolution with strain

In Fig. 4, we show a log–log plot of strain rate *vs.* volumetric strain for the entire suite of experiments. In contrast to the theoretical prediction, these do not show linear relations. Instead, strain rate seems to decrease more slowly than the predictions based on a regular aggregate of mono-sized particles. In comparison to previous studies on pressure solution in aggregates of rock salt and quartz (Spiers and Schutjens, 1990; Spiers et al., 1990), the slopes in our volumetric-strain *vs.* strain-rate curves are very similar, showing a low dependence that increases with increasing strain (i.e. n decreases from −0.5 to values of ~−4, see also Table 2). The determination of the slope at the initial part of the experiment is hindered by the high compaction rate during this phase, limiting the number of data points, whereas the slope towards the end of the experiment is troublesome because of electronic noise in the data. In general, however, the values of the slopes fit roughly within the range predicted for aggregates with grain shapes varying between cubical and spherical (i.e. $n=-1$ for truncation of spheres and $n=-4$ for sharp, cusp-shaped grain edges). The increasing n-values for all experiments seem to suggest that, on average, particle shape changes from more spherical in the beginning to more angular towards the end of the experiments, which is in contrast to the expectation that sharp, angular contacts under high local stress should be preferentially removed by pressure solution. There are a number of possible explanations for this apparent discrepancy. First, the theoretical models assume that the aggregates deform isotropically, *i.e.* they do not develop a fabric during deformation. However, due to the uniaxial nature of the experiment, a grain shape preferred orientation should develop orthogonal to the normal stress. The development of grain shape preferred orientation has a direct effect on the development of the average grain-to-grain contact area and thus on the dependence of strain rate on volumetric strain (Schutjens, 1991). Second, the compaction process could by influenced by the distribution, thickness and physical nature of the grain boundary fluid interface. All these could be complex functions of the local normal stress and volumetric strain (Rutter, 1983; Spiers and Schutjens, 1990; Schutjens, 1991). Third, the theoretical models are, strictly speaking, only valid for the initial part of the experiments (i.e. up to a volumetric strain of ~20%, (Spiers and Schutjens, 1990).

Finally, the theoretical models are based on aggregates of mono-sized particles. The presence of a distributed grain size will have a significant effect on the local stress field and thus on the compaction rate. Also, since smaller grains are more prone to compaction by pressure solution, the dependence of strain rate on average contact area and hence volumetric strain will be different when a larger number of smaller grains are present and should not be log-linearly related.

5.2. Grain size dependence

Theoretical models for pressure solution predict a grain size dependence p of strain rate of 1 or 3 depending on the rate-controlling

mechanism (i.e. $p=1$ for dissolution at the grain boundary, $p=3$ for diffusion out of the grain boundary, and $p=1$ for precipitation on the pore wall). The kinetics of dissolution and precipitation are several orders of magnitude higher than the kinetics of diffusion in the case of salt at room temperature, so diffusion should be the rate-limiting process. In Fig. 5 we show strain rate *vs.* the average grain size (derived from sieve sizes) for different values of volumetric strain. Experiments are compared at equivalent volumetric strain since this implies comparable "geometry" (i.e. packing and contact area) for different aggregates.

The grain size exponents thus determined deviate from the theoretical value of 3, which is consistent with previous studies that analyze grain size dependence (Spiers et al., 1990; Dewers and Hajash, 1995; Niemeijer et al., 2002). The deviation from $p=3$ increases with an increase in volumetric strain (Fig. 5). Part of the discrepancy can be explained by the idealized packing geometry and grain shape assumed in the theory leading to $p=3$. For realistic grain shapes, the packing geometry varies with grain size distribution, angularity and aspect ratio of the grains. Another explanation might be a preferred particle orientation leading to the development of a shape fabric during the uniaxial experiment.

The data of Fig. 5 indicate the problems associated with comparison of pressure solution experiment and theory. Our experiments focus on grain size distribution, but a detailed comparison is difficult due to concomitant variations in particle packing geometry, which varies from sample to sample even at constant volumetric strain. This is also evident from the dependence of strain rate on strain, which suggests different grain shapes and/or packing for the different experiments. A solution to this problem would be either to use perfect spheres as sample material (as attempted by Rossi et al., 2007) or to numerically model a large number of grains using realistic grain geometry to derive grain size exponents. Clearly, for experimental work on natural materials where dissolution, diffusion and/or precipitation rates are unknown or of the same order of magnitude, determining the rate-limiting process from the grain size exponent will be problematic.

5.3. Effect of a distributed grain size

In Fig. 6, we show volumetric strain rate as a function of the coefficient of variation of the grain size distribution for the four samples with a similar mean grain size (p1477, p1478, p1647 and p2030). Narrower size distributions have a smaller coefficient of variation than

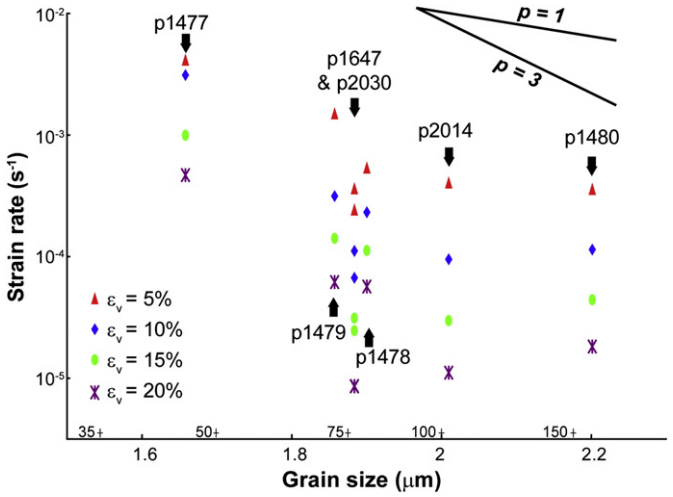

Fig. 5. Plot of strain rate vs. average grain size in log–log space for constant values of volumetric strain (5, 10, 15 and 20%). The slope of a linear fit through the data would indicate the grain size exponent which has a theoretical value of 3 for diffusion-controlled pressure solution.

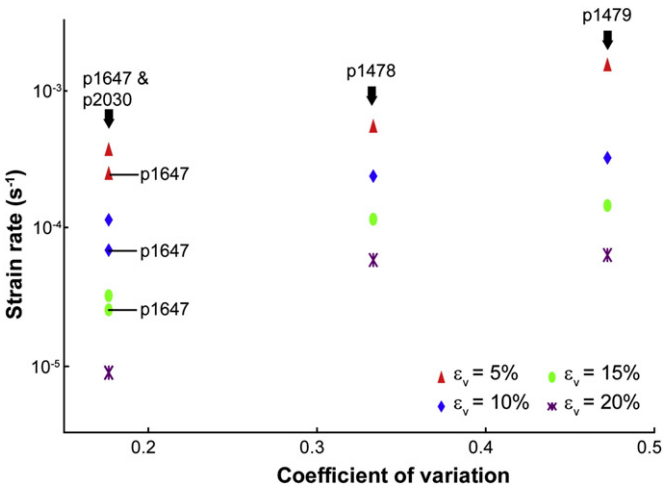

Fig. 6. Semi-log plot of strain rate vs. the coefficient of variation (standard deviation/average value) showing the increase in pressure solution rates with increasingly wider grain size distributions.

wider size distributions. These data clearly show that compaction rate varies with grain size distribution. Compaction rate is larger by up to one order of magnitude or more for poorly sorted grains and the effect decreases with increasing compaction. These data are consistent with the idea that smaller grains allow for an initially higher compaction rate, due to the cubic dependence of compaction rate on grain size. In order to test this hypothesis, we performed one experiment using a bi-modal grain size distribution (50 wt.% 38–53 μm + 50 wt.% 106–212 μm, p2014, see Table 1). Indeed, this experiment shows a high initial compaction rate, similar in magnitude to experiment p1477 which has only the small grain size fraction (see Fig. 2c). The compaction rate drops after the initial high rate to a background value similar or slight smaller than the experiment with only the large grain size fraction (p1480).

Clearly, the width of the grain size distribution has a major effect on the overall compaction of the aggregate. The presence of small grains leads to high initial compaction rates due to the cubic dependence of pressure solution rates on grain size. This leads to a distribution of compaction rates similar to the grain size distribution and the overall macroscopic (measured) compaction rates is some average value of this distribution. With ongoing compaction, the smallest grains will stop compacting, either because they are completely dissolved or because the contact area is too large, effectively decreasing the macroscopic compaction rate.

6. Implications

Grain size distributions for natural rocks and fault gouges follow a power-law or fractal size distribution (Sammis et al., 1986). Therefore, if pressure solution is active in these rocks, the spatiotemporal location of the widest distribution in grain size will be the site of the highest deformation rate by pressure solution. As compaction proceeds and porosity decreases, low porosity zones will tend to form and thereby limit fluid flow locally. If diffusion is not the rate limiting mechanism of pressure solution, material from high porosity zones with initially more narrow grain size distributions, will diffuse into the low porosity zones, where fluid flow rates are lower, allowing the transported material to precipitate. This extra cementation would tend to increase the contrast in porosity, further limiting fluid flow and potentially creating pockets or zones of high pore pressures. The increased porosity reduction due to both effects will lead to significantly higher sealing and healing rates than predicted using "classical" pressure solution models. The high pore pressure pockets could initiate unstable frictional slip. Accounting for these effects may be important in modeling the evolution of hydrocarbon reservoirs, regional fluid flow and the processes of fault healing, sealing and pore pressure evolution during the seismic cycle (Renard et al., 2000; Gratier et al., 2003; Fitzenz et al., 2007)}.

Acknowledgements

We thank two anonymous reviewers for their suggestions and comments which helped improve this paper. This work was supported by NSF grants EAR-0510182 and ANT-0538195 and by the Netherlands Organisation for Scientific Research (N.W.O.) grant 825.06.003. This support is gratefully acknowledged.

References

Bernabé, Y., Evans, B., 2007. Numerical modelling of pressure solution deformation at axisymmetric asperities under normal load. Spec. Publ. — Geol. Soc. Lond. 284, 1185–1205. doi:10.1144/SP1284.1113.

Dewers, T.A., Hajash, A., 1995. Rate laws for water-assisted compaction and stress-induced water–rock interaction in sandstones. J. Geophys. Res. 100, 13093–13112.

Fitzenz, D.D., Jalobeanu, A., Hickman, S.H., 2007. Integrating laboratory creep compaction data with numerical fault models: a Bayesian framework. J. Geophys. Res. 112. doi:10.1029/2006JB004792.

Gratier, J.-P., 1993. Le fluage des roches par dissolution–cristallisation sous contrainte, dans la croûte supérieure. Bull. Soc. Geol. Fr. 164, 267–287.

Gratier, J.-P., Favreau, P., Renard, F., 2003. Modeling fluid transfer along California faults when integrating pressure solution crack sealing and compaction processes. J. Geophys. Res. 108. doi:10.1029/2001JB000380.

Gundersen, E., Renard, F., Dysthe, D.K., Bjørlykke, K., 2002. Coupling between pressure solution creep and diffusive mass transport in porous rocks. J. Geophys. Res. 107. doi:10.1029/2001JB000287.

Mullis, A.M., 1991. The role of silica precipitation kinetics in determining the rate of quartz pressure solution. J. Geophys. Res. 96, 10007–10013.

Niemeijer, A.R., Spiers, C.J., Bos, B., 2002. Compaction creep of quartz sand at 400–600 °C: experimental evidence for dissolution-controlled pressure solution. Earth Planet. Sci. Lett. 195, 261–275.

Raj, R., 1982. Creep in polycrystalline aggregates by matter transport through a liquid phase. J. Geophys. Res. 87, 4731–4739.

Renard, F., Park, A., Ortoleva, P., Gratier, J.-P., 1999. An integrated model for transitional pressure solution in sandstones. Tectonophysics 312, 97–115.

Renard, F., Gratier, J.-P., Jamtveit, B., 2000. Kinetics of crack-sealing, intergranular pressure solution, and compaction around active faults. J. Struct. Geol. 22, 1395–1407.

Revil, A., Leroy, P., Ghorbani, A., Florsch, N., Niemeijer, A.R., 2006. Compaction of quartz sands by pressure solution using a Cole–Cole distribution of relaxation times. J. Geophys. Res. 111. doi:10.1029/2005JB004151.

Rossi, M., Vidal, O., Wunder, B., Renard, F., 2007. Influence of time, temperature, confining pressure and fluid content on the experimental compaction of spherical grains. Tectonophysics 441, 47–65. doi:10.1016/j.tecto.2007.1005.1001.

Rutter, E.H., 1976. The kinetics of rock deformation by pressure solution. Philos. Trans. R. Soc. Lond. Abstr. 283, 203–219.

Rutter, E.H., 1983. Pressure solution in nature, theory and experiment. J. Geol. Soc. (Lond.) 140, 725–740.

Sammis, C.G., Osborne, R.H., Anderson, J.L., Bandert, M., White, P., 1986. Self-similar cataclasis in the formation of fault gouge. Pure Appl. Geophys. 124, 53–78.

Schutjens, P.M.T.M., 1991. Experimental compaction of quartz sand at low effective stress and temperature conditions. J. Geol. Soc. (Lond.) 148, 527–539.

Shimizu, I., 1995. Kinetics of pressure solution creep in quartz: theoretical considerations. Tectonophysics 245, 121–134.

Spiers, C.J., Brzesowsky, R.H., 1993. Densification behaviour of wet granular salt: theory versus experiment. Seventh Symposium on Salt 1. Elsevier, pp. 83–92.

Spiers, C.J., Schutjens, P.M.T.M., 1990. Densification of crystalline aggregates by fluid phase diffusional creep. In: Barber, D.J., Meredith, P.G. (Eds.), Deformation Processes in Minerals, Ceramics and Rocks. Unwin Hyman, London, pp. 334–353.

Spiers, C.J., Schutjens, P.M.T.M., Brzesowsky, R.H., Peach, C.J., Liezenberg, J.L., Zwart, H.J., 1990. Experimental determination of constitutive parameters governing creep of rocksalt by pressure solution. Deformation Mechanisms, Rheology and Tectonics. In: Geological Society Special publication, vol. 54. The Geolocial Society of London, London, pp. 215–227.

Spiers, C.J., De Meer, S., Niemeijer, A.R., Zhang, X., 2004. Kinetics of rock deformation by pressure solution and the role of thin aqueous films. In: Nakashima, S., Spiers, C.J., Mercury, L., Fenter, P.A., Hochella, J.M.F. (Eds.), Physicochemistry of Water in Geological and Biological Systems, Frontiers Science Series. Universal Academy Press, Inc., Tokyo, Japan, pp. 129–158.

Yasuhara, H., Elsworth, D., Polak, A., 2003. A mechanistic model for compaction of granular aggregates moderated by pressure solution. J. Geophys. Res. 108. doi:10.1029/2003JB002536.